Solution Structure of the Aqueous Model Peptide *N*-Methylacetamide

Susan K. Allison,*,† Simon P. Bates,† Jason Crain,†,‡ and Glenn J. Martyna‡

School of Physics, University of Edinburgh, Mayfield Road, Edinburgh EH9 3JZ, United Kingdom, and IBM T. J. Watson Research Center, Yorktown Heights, New York, 10598

Received: July 3, 2006; In Final Form: August 18, 2006

Classical molecular dynamics simulations of aqueous *N*-methylacetamide (NMA) have been performed across a concentration range at 308 K. This peptidic fragment molecule is a useful model for investigating water/peptide hydrogen bond competition. The simulations predict considerable NMA self-association even at low concentrations with a concentration-dependent increase in the ratio of branched to linear clusters. Water-mediated NMA contacts are a feature of this regime, manifested by an unexpected increase in the number of short NMA oxygen contacts arising from water bridge motifs. In contrast, bulk water structure is significantly disrupted by the addition of even small quantities of NMA. With increases in NMA concentration water molecules become progressively more isolated, forming dimers and trimers hydrogen-bonded to NMA. The mixture in this concentration regime may therefore offer a minimal model system for certain structural properties of interior water buried in protein cavities and hydrogen-bonded to mainchain peptide groups.

1. Introduction

The role of water in influencing the structure and function of biological macromolecules is not yet completely understood. One route to understanding the complex processes involved lies in studying suitable model systems. *N*-Methylacetamide (NMA) is one of the simplest molecules containing the peptide linkage and has the advantage of being small enough to be accessible by both current experimental and computational techniques. The pure substance forms interpeptide hydrogen bonds that are known to stabilize polypeptide secondary structures.[1] However, ab initio simulations reveal that solvation has a large effect on the strengths of these bonds,[2] and there are still open questions regarding the competition between interpeptide and peptide−water hydrogen bonds and their contribution to protein folding and stability.[3]

Schellman's[4] initial investigation of peptide hydrogen bond energetics suggested that helix formation was driven by the enthalpy of the hydrogen bond. The use of NMA as a model for proteins was established by Klotz and Franzen[5] in 1962 whose work cast doubt on the importance of hydrogen bonding in proteins. Their infrared spectra indicated that the stability and strength of the interpeptide hydrogen bond formed in NMA dimerization were much less than expected. Subsequently Kauzmann proposed that the driving force for protein folding was hydrophobicity.[6]

More recent work by Ludwig and co-workers shows evidence of strong hydrogen bond cooperativity in liquid NMA[7,8] that would not have been apparent in Klotz and Franzen's dimerization study. Raman and Fourier transform infrared (FTIR) spectra[9] indicate that pure liquid NMA forms long and short oligomeric chains with both parallel and antiparallel molecular orientations. The structure of the pure liquid at 308, 373, and 458 K has recently been discussed in detail by Whitfield et al.[10,11] On the basis of classical molecular dynamics (MD) simulations they show that local alignments of inter- and intrachain segments account for the main features of the radial and angular distribution functions. In addition to strong hydrogen bonding through the amide group the NMA molecule is also capable of forming "weak" or "improper" hydrogen bonds between oxygen and methyl hydrogen atoms. Whitfield et al.[11] identified two types of "improper" contacts:

(i) "Interchain" interactions cause distinct hydrogen-bonded chains to loosely associate into planar sheets. These sheets bear a resemblance to the hydrogen-bonding motif transverse to polypeptide chains in the β-sheet form of secondary protein structure.[10]

(ii) "Intrachain" interactions between strongly hydrogen-bonded NMA molecules were also identified.

Aqueous NMA has been more extensively studied by computer simulation than by experiment. The majority of work focuses on the effect of hydration on vibrational frequencies, in particular the amide I mode of NMA.[12−14] Ab initio calculations have been used to investigate the cis−trans isomerization pathway of a single NMA molecule in vacuo and explicit water solvent.[15] Of more relevance to the current study are FTIR spectroscopy results that show that self-associated NMA structures are favored in the aqueous solution and that water prefers to donate to the NMA carbonyl group.[3] The strong hydrogen bonds that form between the amide and carbonyl functional groups of the peptide linkage and between these groups and water have been the subject of extensive research both in NMA and in other biomimetic systems. However, less is known about the weaker interactions that exist between these groups and methyl hydrogens. Zhang et al.[16−18] are one of the few groups to have presented structural data on the weak interactions in aqueous NMA systems on the basis of classical MD simulations.

In this paper we study aqueous NMA across the full concentration range. This allows access to two important limiting cases: First, that of dilute NMA in water offers a model system relevant to the hydration of the peptide group and gives insight

* Author to whom correspondence should be addressed. Phone: +44-(0)1316506798. E-mail: susie.allison@ed.ac.uk.
† University of Edinburgh.
‡ IBM T. J. Watson Research Center.

10.1021/jp064154y CCC: $33.50
Published on Web 09/27/2006

TABLE 1: Energy Parameters for Aqueous NMA Simulations

atom	partial charge (*e* units)	ϵ (kcal mol^{-1})	σ (Å)
C_C	0.27	0.0800	4.1200
C_N	0.11	0.0800	4.1200
C	0.51	0.1100	4.0000
N	−0.47	0.2000	3.7000
O	−0.51	0.1200	3.4000
H	0.31	0.0460	0.4490
H_C	0.09	0.0220	2.6400
H_N	0.09	0.0220	2.6400
O_W	−0.82	0.1848	3.5532
H_W	0.41	0.0100	0.9000

into the persistence and structure of hydrogen-bonded oligomers in aqueous solution. At the opposite extreme, concentrated NMA represents a simple system where water exists in an environment rich in peptide groups. Though largely unexplored this concentration regime may be relevant to the issue of *interior* or *buried* water molecules trapped in the internal cavities of many proteins and hydrogen-bonded to the main chain backbone.[19] Specifically, we seek first to determine via quantitative analysis of hydrogen-bonded cluster populations as well as radial and generalized two-dimensional (2D) distribution functions the way in which conventional and weak methyl-donating hydrogen bonding between the NMA peptide groups is disrupted on dilution in water. Second, we wish to explore the hydration structure of NMA molecules as a function of concentration and, third, to explore the structure of water in these mixtures and the progressive changes that result from increasing the peptide group concentration.

2. Computational Details and Methodology

2.1. Simulation Details. We have performed classical MD simulations for a series of NMA and water mixtures across a concentration range. The simulations were carried out using the DL_POLY package[20] in conjunction with fully flexible all-atom CHARMM22[21] and F3C[22] force fields for NMA and water, respectively. These potential parameters, shown in Table 1, have been previously shown to give good predictions of the single-component liquid structure.[11,22] However, the degree of dipole coupling may be underestimated as polarizability is neglected in these models.[23] Cross terms for NMA−water van der Waals interactions were calculated using geometric combination rules.[22] Cubic simulation boxes with side lengths of approximately 30 Å were used for all concentrations. Periodic boundary conditions were applied and electrostatic interactions were calculated using the Ewald summation method.

Initially, randomly oriented water and *trans*-NMA molecules were placed on a lattice. The density of the mixture varies with composition and is set to the correct experimental density[24] for the state point $T = 308.15$ K, $P = 1$ bar. Each concentration was equilibrated before commencing a data collection run of 1 ns using a 0.5 fs integration time step. The *NVT* ensemble was implemented using the Nosé−Hoover thermostat with a relaxation constant of 0.05 ps. Trajectory snapshots were saved every 0.1 ps for analysis. Larger simulation boxes of side lengths of 60 Å were used to confirm that 30 Å was sufficient to ensure finite size effects had no quantitative effects upon results.

2.2. Radial and Multidimensional Distribution Functions. The standard radial distribution function $g(r)$ is commonly used to characterize the short and intermediate range order of molecular liquids. It also serves as a useful point of comparison between the results of experimental and simulation studies. However, by collapse of three-dimensional (3D) space onto a one-dimensional function, information is inherently lost with the result that some structural features are disguised. It is therefore useful to consider multidimensional distribution functions, which with their extra degrees of freedom are capable of distinguishing between different structural motifs.

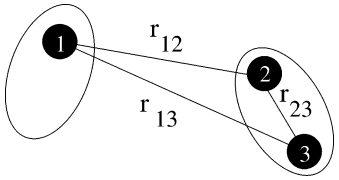

Figure 1. Schematic of a pair of molecules illustrating the atomic sites used in the definition of the multidimensional distribution functions $g_2(r_{12}, \cos\theta_{123})$.

Two-dimensional distributions can be constructed as described by Whitfield et al.[11] The methodology is described below with reference to Figure 1. Atoms 2 and 3 are connected by covalent bonds since they belong to the same molecule, and therefore their average separation, $\langle r_{23}\rangle$, is well defined. A radial-angular distribution, $g_2(r_{12}, \cos\theta_{123})$ can be defined by the distance between atoms 1 and 2 and the cosine of the angle formed by the three atoms with atom 2 at the vertex of the triangle. Thus radial features belonging to the same $g(r)$ peak but arising from different angular correlations can be easily distinguished. This distribution is especially useful in hydrogen-bonded systems such as NMA−water as it is capable of illustrating the angular spread of strong and weak hydrogen bonds. The standard radial distribution function can be recovered by integration

$$g(r_{12}) = \frac{1}{2}\int_{-1}^{1} g_2(r_{12}, \cos\theta_{123})\, \mathrm{d}(\cos\theta_{123}) \qquad (1)$$

Contour plots of these multidimensional distribution functions can be more easily interpreted than plots of the 3D surface. In all plots shown the initial contour height is $g(r) = 1$; hence these plots depict enhanced structural features only. Analysis and visualization of simulation trajectories enables identification of structural motifs corresponding to $g(r)$ and $g_2(r, \cos\theta)$ peaks.

2.3. Cluster Analysis. "Clusters" are defined as single species groups of molecules connected by a continuous strong hydrogen bond network. We have previously employed this methodology in a series of papers on aqueous alcohol solutions.[25,26] Strongly hydrogen-bonded molecules satisfy two geometric requirements:

(i) The donated hydrogen is within r_{AH} of the accepting atom, where r_{AH} is defined as the first minimum in the relevant radial distribution function $g(r_{AH})$ between the acceptor atom, A, and the donated hydrogen, H.

(ii) The angle formed between the acceptor, hydrogen, and donor atoms deviates from 180° by less than 40°.

The suitability of these geometric rules was confirmed both by looking at the angular distribution of the hydrogen-bonded peaks in the 2D correlation functions and by testing the sensitivity of the results to a variation in the criteria. The angular cutoff chosen was the strictest definition that preserved the hydrogen-bonding behavior of NMA in our previous study of the pure liquid.[11] For internal consistency the same angular cutoff was used for water−NMA, NMA−water, and water−water hydrogen bonding in the aqueous solutions. The consequences of this choice were investigated by comparing the results obtained using a variety of angular cutoffs and showed that the qualitative trends obtained are insensitive to small variations in the cutoff angle. Unfortunately, there is no universally accepted definition of the angular criterion for hydrogen bonding. Mezei and Beveridge[27] define their "strong"

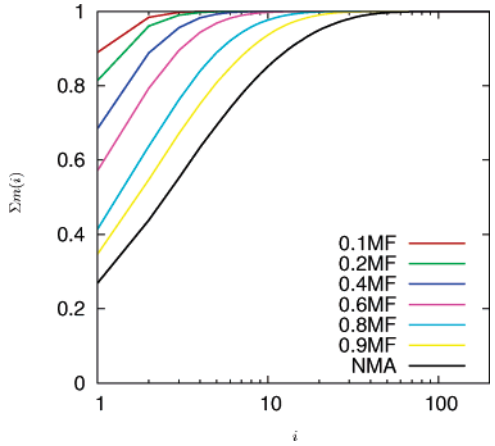

Figure 2. Cumulative NMA cluster frequency, $\Sigma m(i)$, as a function of cluster size, i, for pure NMA and a range of aqueous NMA solutions.

hydrogen-bonded angular cutoff as a deviation from 180° of less than 45°, although it is more common to only permit water−water hydrogen bonds to deviate by 30° from linear.[28] Results for lower concentrations are most affected by variations in the water−water angular cutoff. In our simulations using a cutoff of 40° results in identifying 20% of water molecules in the 0.1 mole fraction (MF) NMA mixture as singletons (forming no hydrogen bonds) instead of the 24% identified when a cutoff of 30° is applied.

When plotting cluster distribution histograms we plot the number of clusters of a size i, $m(i)$, as a fraction of the total number of clusters, M, where $M = \sum_i m(i)$.

3. Results and Discussion

In this section results are presented for the structural changes that occur upon hydration of NMA. Rather than show all pair correlation functions we select only those that exemplify particular structural features. Figure 4 includes a snapshot from the simulation of a 0.2 MF solution, which illustrates the atomic naming conventions that we have adopted throughout. The results are ordered in terms of the types of interspecies interactions present in the mixture. First we consider the disruptive effect of water on the NMA intermolecular chain structure. We then detail the interactions between different species, considering both strong and weak (improper) hydrogen bonding. To conclude the results section we focus our attention on the structure of water in the aqueous solutions.

3.1. Hydration of NMA Chains. The distribution of cluster sizes of NMA molecules in the pure liquid and a selection of aqueous solution concentrations is illustrated in Figure 2. It shows that hydration breaks up the NMA chains, as demonstrated by a depletion of long-chain structures and an increased proportion of monomers and dimers upon increasing the water content of the solution. A significant degree of hydrogen-bonded association remains between NMA molecules at the lowest concentrations explored. It is clear that dimers and trimers are present in significant proportions even in the 0.1 MF solution. At this concentration about 10% of the NMA molecules have hydrogen-bonded NMA neighbors. Corroborative evidence for this degree of self-association can be obtained from the coordination numbers shown in Table 2 and the 2D radial-angular distribution functions of, for example, $g_2(r_{ON}, \cos\theta_{ONH})$. These functions are illustrated in Figure 3, for representative (a) weak, 0.4 MF, and (b) concentrated, 0.9 MF, aqueous NMA solutions. Figure 3 implies order up to trimers in aqueous solution.

TABLE 2: Coordination Numbers for Aqueous NMA Solutions Calculated by Integrating $g(r)$ out to Its First Minimum

$g(r)$	water	0.1	0.2	0.4	0.6	0.8	0.9	NMA
OH		0.15	0.27	0.43	0.58	0.79	0.89	0.98
ON		0.16	0.25	0.46	0.61	0.82	0.91	1.04
OO[a]		0.93	1.42	1.74	2.02	2.23	2.30	2.08
OO_W		1.85	1.60	1.16	0.77	0.38	0.20	
OH_W		1.75	1.49	1.11	0.75	0.37	0.19	
O_WH		0.75	0.73	0.53	0.41	0.24	0.11	
O_WN		0.63	0.62	0.49	0.43	0.24	0.11	
O_WO_W	4.98	4.20	3.61	2.65	1.75	0.82	0.39	
O_WH_W	1.90	1.71	1.53	1.19	0.81	0.39	0.19	
OH_C[b]		4.56	5.28	6.09	6.64	7.07	7.25	7.42
OH_N[b]		4.45	5.11	5.92	6.42	6.83	7.15	7.15
O_WH_C[b]		4.06	3.05	1.81	0.99	0.40	0.19	
O_WH_N[b]		4.18	3.20	1.91	1.05	0.44	0.21	

[a] $g(r_{OO})$ was integrated out to its first maximum. [b] $g(r)$ functions for methyl hydrogens were integrated out to 4 Å.

Further insight into the breakup of NMA chains on hydration is found by examining the correlation functions for oxygen atoms on NMA molecules, $g(r_{OO})$ and $g_2(r_{OO}, \cos\theta_{OOC})$, as shown in Figure 4. In the pure liquid, the first peak of this function, at 4.9 Å, is attributed to the oxygen−oxygen separation of NMA molecules connected by a strong hydrogen bond, with the low-r wing providing evidence for a range of NMA−NMA interchain close contact geometries as shown by Whitfield et al.[11] A plausible hypothesis for the hydration process of NMA chains might involve water molecules first hydrating the chain ends, leaving the pure NMA intermolecular structure reasonably intact at high concentrations. Subsequently, we might expect water molecules to be dispersed between the NMA chains, thus pushing the chains apart. Consequently, this would lead to a decrease in the height of the low-r wing of $g(r_{OO})$. Figure 4c shows $g(r_{OO})$ for pure NMA together with a range of solution concentrations and illustrates, somewhat surprisingly on first sight, that the low-r wing is enhanced on dilution, even at the lowest concentrations explored. The trend is clear in the joint radial-angular distributions. Figure 4a showing $g_2(r_{OO}, \cos\theta_{OOC})$ for the dilute 0.1 MF mixture has more intensity at low r than its concentrated counterpart shown in Figure 4b. The enhancement of this "interchain" correlation at concentrations where almost all the NMA molecules have no hydrogen-bonded neighbors of their own species indicates that water−NMA interactions must be responsible for promoting close NMA−NMA contacts. NMA molecules are not only able to form strong hydrogen bonds with their own species but also with water molecules. This can result in configurations where one or more water molecules form a hydrogen-bonded "bridge" between two NMA molecules as illustrated in Figure 4. These bridge structures promote close contact between the connected NMA molecules leading to O−O separations as low as 3 Å, which contribute to the low-r wing of $g(r_{OO})$. This observation illustrates that the addition of water has an unexpected and nontrivial effect on O−O separation in this model peptide and similar motifs may well also be visible in aqueous proteins. The first peak of $g(r_{OO})$ at 4.9 Å diminishes as water is added and seems to have vanished almost completely at the lowest concentrations. We can clearly see why this is so by considering the clustering results illustrated in Figure 2. At 0.2 MF only 10% of the NMA molecules form clusters of three or more molecules and so are able to contribute to this peak. The picture of the hydration process is one of NMA chains breaking up on dilution into isolated molecules and short chains while retaining close OO contacts due to NMA−water interactions.

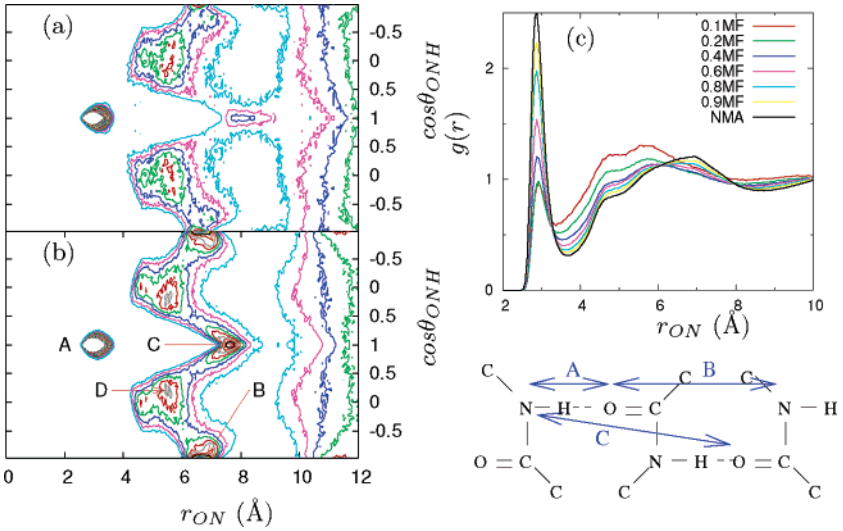

Figure 3. $g_2(r_{ON}, \cos\theta_{ONH})$ for (a) 0.4 and (b) 0.9 MF aqueous solutions. Contour levels start at $g_2(r, \cos\theta) = 1$ (turquoise), increasing in increments of 0.1 up to 5. $g(r_{ON})$ is shown in part c. The schematic (methyl hydrogens not shown) illustrates the structural motifs giving rise to the features of $g_2(r_{ON}, \cos\theta_{ONH})$. (A) Hydrogen-bonded contact between adjacent chain members ("close" dimer contact): $r = 2.9$ Å, $\theta = 0°$. (B) Contribution from the amide and carbonyl groups that do not participate in the hydrogen bond of the NMA dimer ("far" dimer contact): $r = 6.5$ Å, $\theta = 180°$. (C) Close trimer contact: $r = 7.5$ Å, $\theta = 0°$. (D) Interchain contributions. The broad band between 10 and 12 Å arises from a number of inter- and intrachain configurations including the far trimeric contact, tetrameric contacts, and parallel chain contributions.

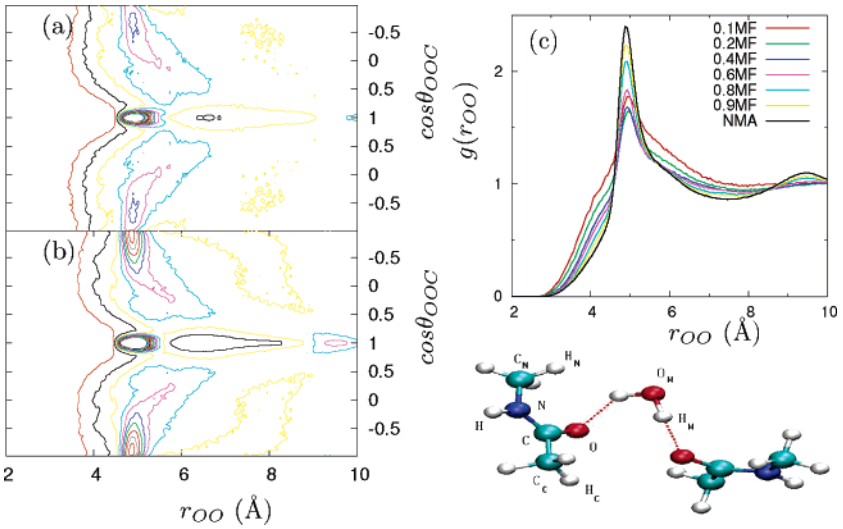

Figure 4. $g_2(r_{OO}, \cos\theta_{OOC})$ for (a) 0.1 and (b) 0.9 MF aqueous solutions. Contour levels start at $g_2(r, \cos\theta) = 0.3$ (orange), increasing in increments of 0.3 up to 5. (c) $g(r_{OO})$ for pure NMA and a selection of its aqueous solutions. Bridges formed by hydrogen-bonded water molecules force close contact between the oxygen atoms of NMA molecules and cause the low-r tail of $g(r_{OO})$ to increase with water MF. Such bridges can be formed by more than one water molecule. A single-molecule "water bridge" is illustrated and annotated with the atomic naming conventions used throughout the text. Atom labels without subscripts belong to NMA molecules. Atoms belonging to water molecules are indicated with a subscript "W".

NMA oxygen atoms are capable of accepting two hydrogen bonds and do so in just less than 10% of cases in the pure liquid. Consequently, these doubly accepting molecules form branch points in hydrogen-bonded chains. It is possible to obtain a rough estimate of the degree of branching of the NMA hydrogen-bonded networks by counting the number of molecules in a given cluster that only have one hydrogen-bonded neighbor. Such molecules are "endpoints" of the cluster. Making the well-justified assumption that a population of *trans*-NMA molecules is unlikely to hydrogen bond to form rings, the number of branches in a given cluster is then equal to the number of endpoints, i.e., 2. Figure 5 presents the variation in the number of endpoints as a function of concentration for three different cluster sizes and an illustrative five-molecule branched cluster. Comparing NMA clusters of like size reveals a trend whereby the average number of branches increases with decreasing NMA concentration. This trend suggests the following theory of hydration of NMA chains: As water is added to the system it is more likely to be inserted into the NMA chains at linear sections. This simply could be due to steric effects. It will be easier for water molecules to approach linear segments of the NMA chain as opposed to branch points.

3.2. NMA−Water Strong Hydrogen Bond Interactions. As discussed in the previous section the addition of water to liquid NMA has an unexpected and nontrivial effect on NMA−NMA interactions due to the formation of hydrogen-bonded water bridge structures. The radial distribution function for contacts between the NMA and water oxygen atoms is shown in Figure 6 and provides insight into the interspecies hydrogen bonding within the liquid. The first peak at 2.7 Å in $g(r_{OO_W})$ corresponds to hydrogen-bonded configurations where the NMA molecule is acting as an acceptor from a neighboring water hydrogen. This is illustrated in the simulation snapshot pictured in Figure 6, with this type of $O-O_W$ interaction labeled as "A".

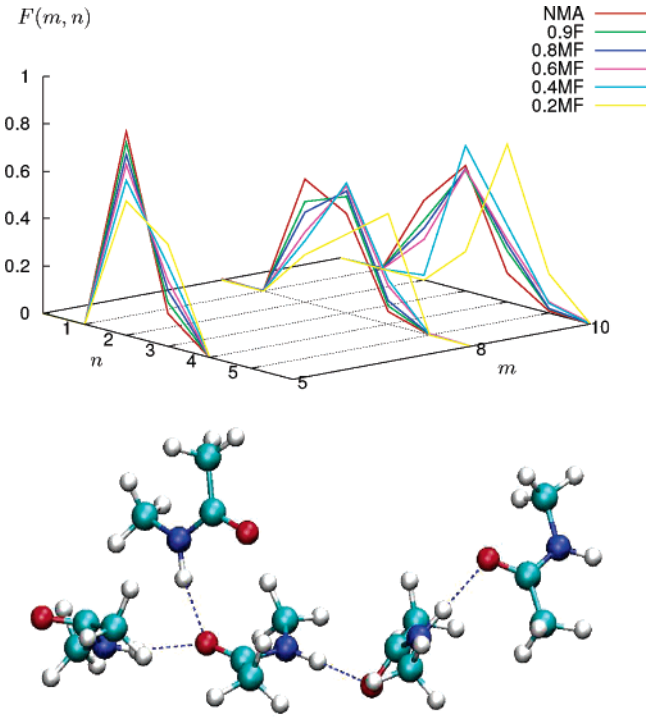

Figure 5. $F(m, n)$, the proportion of the total number of clusters containing m molecules that have n endpoints plotted as a function of m and n for a range of concentrations. The simulation snapshot shows a five-molecule cluster with three endpoints (one branch).

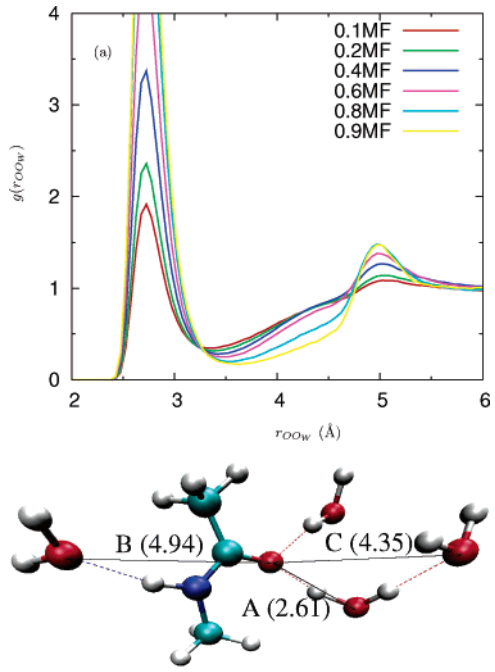

Figure 6. (a) $g(r_{OO_W})$ for aqueous NMA concentrations in the range 0.1 to 0.9 MF and (b) a snapshot taken from a simulation of 0.1 MF aqueous NMA showing a single NMA molecule with its three hydrogen-bonded water neighbors and a second nearest neighbor water connected to the NMA by two hydrogen bonds. Hydrogen bonds donated by the NMA molecule are indicated with a blue dotted line. Those donated by waters are indicated with a red dotted line. The black arrows and letters refer to the interactions described in the text with distances measured in angstroms.

The second distinct peak at 5 Å arises from configurations in which the NMA molecule acts as a hydrogen bond donor (the $O-O_W$ interaction labeled "B" in Figure 6b). This peak broadens to lower r and becomes less distinct as the NMA concentration decreases in the aqueous solutions. It is apparent that a variety of NMA−water structural motifs also contribute to the 5 Å peak of $g(r_{OO_W})$:

(i) water molecules separated by two or three hydrogen bonds from the NMA oxygen (C in Figure 6b),

(ii) water molecules hydrogen-bonded to the NMA donor group (B in Figure 6b), and

(iii) water molecules close to but not necessarily hydrogen-bonded to the NMA donor group (not shown).

Of these, the only molecules contributing to the region between the two peaks are water molecules connected to the NMA molecule by two hydrogen bonds, labeled "C" in Figure 6b. In this region $g(r_{OO_W})$ clearly increases as the NMA mole fraction decreases. The NMA−water structural motifs described above explain the forms of the other interspecies distributions that are not explicitly shown in this paper such as $g(r_{NO_W})$.

3.3. Methyl Group Interactions. In addition to the strong hydrogen-bonding interactions between water molecules and the atoms of the peptide linkage, it has been reported that methyl-donated improper hydrogen bonds in the pure liquid stabilize interchain interactions.[11] On the basis of molecular dynamics simulations and measurements of NMR spectra Zhang et al.[16−18] report the presence of weak or improper hydrogen-bonded contacts in the aqueous solution.

On hydration of pure NMA the coordination numbers and spatial distributions of the methyl hydrogens change in a manner consistent with the breakup of the NMA chains. Weak interactions between the methyl hydrogens and the carbonyl oxygen continue to be apparent wherever there are strongly hydrogen-bonded NMA chains or dimers. Figure 7a and 7b show joint radial-angular distributions for interactions of the two distinct types of methyl hydrogen with the water oxygen atom for a 0.1 MF solution. These provide evidence for the existence of improper hydrogen bonds between water and methyl hydrogens. Hydrogens belonging to the methyl group on the carbonyl side of the NMA molecule approach the water oxygens nearly 1 Å more closely than hydrogens belonging to the methyl group attached to the amide functional group. Additionally the H_C atom distribution is spread out over a much wider radial range than that of H_N but has a more distinct angular distribution as is also observed for the interactions of the methyl groups with the NMA oxygen (Supporting Information). Due to the zigzag conformation of the NMA molecules the methyl group attached to the carbonyl carbon, Me_C, points toward the accepting water molecule while that attached to the nitrogen, Me_N, points away. This geometry brings the Me_C group into close enough proximity to the water oxygen that it becomes orientationally contrained and consistently points one of its methyl hydrogens toward the water molecule. These pinning interactions are within the angular and distance contraints often used to define improper hydrogen bonding.[30] Conversely, Figure 7a shows no such "pinning", indicating that the Me_N group is able to rotate freely. This structural interpretation not only provides a convincing explanation of our own results but also for those of Zhang et al. Both their NMR experiments and statistical analysis of simulation trajectories indicated that there were more H_C-O than H_N-O contacts.

3.4. Water−Water Interactions. In this final results section we investigate the influence of NMA on the hydrogen bond network in water. Pure water's tetrahedral intermolecular structure is characterized by the second peak of $g(r_{O_WO_W})$ at approximately 4.5 Å as shown in Figure 8. Since this peak arises from second nearest neighbor contacts, water molecules participating in hydrogen-bonded clusters of less than three

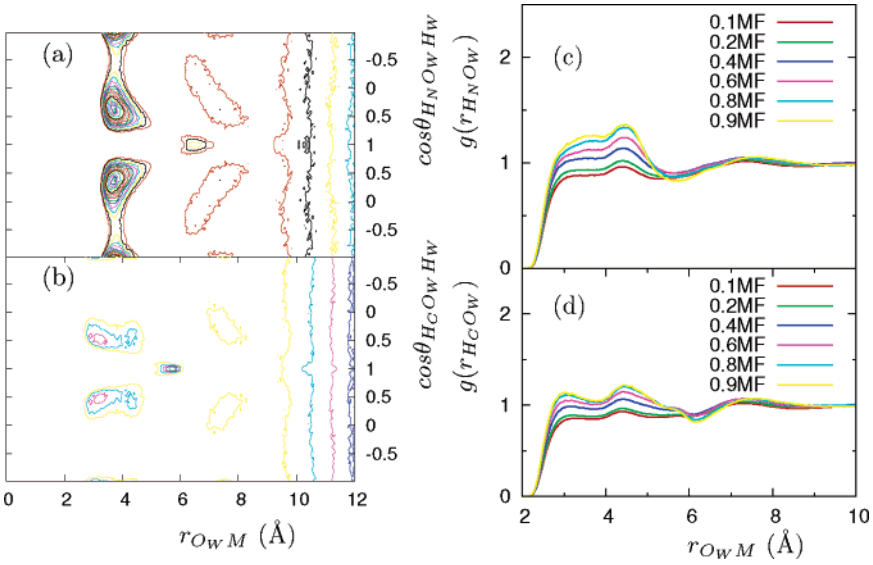

Figure 7. (a) $g_2(r_{H_NO_W}, \cos\theta_{H_NO_WH_W})$ and (b) $g_2(r_{H_CO_W}, \cos\theta_{H_CO_WH_W})$ for 0.1 MF aqueous NMA. Contour levels start at $g_2(r, \cos\theta) = 1$ (orange contour in part a, yellow contour in b) increasing in increments of 0.1 up to 5. Parts c and d illustrate the corresponding radial distributions for $g(r_{H_NO_W})$ and $g(r_{H_CO_W})$, respectively.

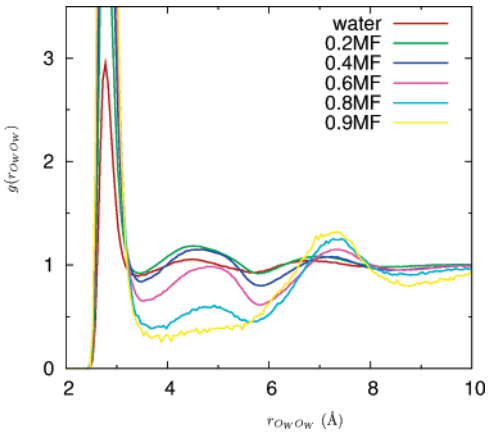

Figure 8. $g(r_{O_WO_W})$ for water and aqueous NMA mixtures between 0.2 and 0.9 MF

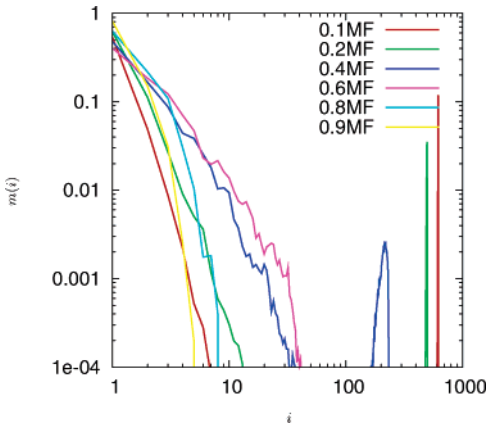

Figure 9. Cluster frequency as a function of cluster size for water molecules in aqueous NMA solutions of concentrations between 0.2 and 0.9 MF. Note that the maximum possible cluster size depends on the total number of water molecules in the simulation, which varies as a function of concentration. The spikes in the cluster distributions for the 0.2 and 0.4 MF solutions indicate clusters containing all the water molecules in the system.

molecules will not contribute to this peak. As the mole fraction of water in the mixtures decreases this peak diminishes until it is barely present in the most concentrated solution (0.9 MF). Therefore in the concentrated solutions water molecules are isolated or form dimers rather than clusters. Corrobative evidence comes from the clustering analysis for water molecules, which suggests that in the 0.9 MF solution over 90% of the water molecules are isolated (67%) or form half of a dimer (25%) as shown in Figure 9. Significant proportions of water molecules are isolated in all the high-concentration mixtures, indicating that this may be a good model system in which to explore the structure and dynamics of water in peptide-rich environments such as those found in the interior of proteins.[19] Figure 10 shows that the hydrogen-bonded interactions of the buried water present in the bovine pancreatic trypsin inhibitor (BPTI) protein[29] bear similarities to the interactions of isolated water molecules in concentrated NMA solutions.

As the 4.5 Å $g(r_{O_WO_W})$ peak disappears with increasing NMA concentration a new peak forms at about 7 Å, a slightly larger radial separation than the third neighbor shell of pure water. This new peak arises from second nearest neighbor contacts; however, in this case the bridging molecule is not water but NMA. The water−NMA intermolecular structure is not as well ordered as the structure of pure water; hence the correlations are not restricted to a narrow angular range. In the higher-concentration solutions, the radial and angular ranges of this peak are also broadened by the inclusion of contributions from structural configurations such as water trimers.

In a truly tetrahedral network each vertex is of degree 4: For the water network this translates as each water oxygen accepting two hydrogen bonds while both water hydrogens are donated to other molecules. In practice this ideal network structure will be rare in liquid water as hydrogen bonds continually break and form. However, the majority of water molecules in the pure liquid will, on average, be four-coordinated. In the aqueous simulations this is only true of water molecules in mixtures with an NMA concentration of less than 0.1 MF. (It is worth noting that a 0.1 MF solution is about 4 M.). At concentrations greater than 0.1 MF there are more water molecules accepting a single hydrogen bond from other waters than those that accept two. It is apparent that the hydrogen bond network of pure water is significantly disrupted even at these concentrations, which are the lowest we have investigated thus far. The disruption is clear upon visualization of the simulation trajectory. At very high

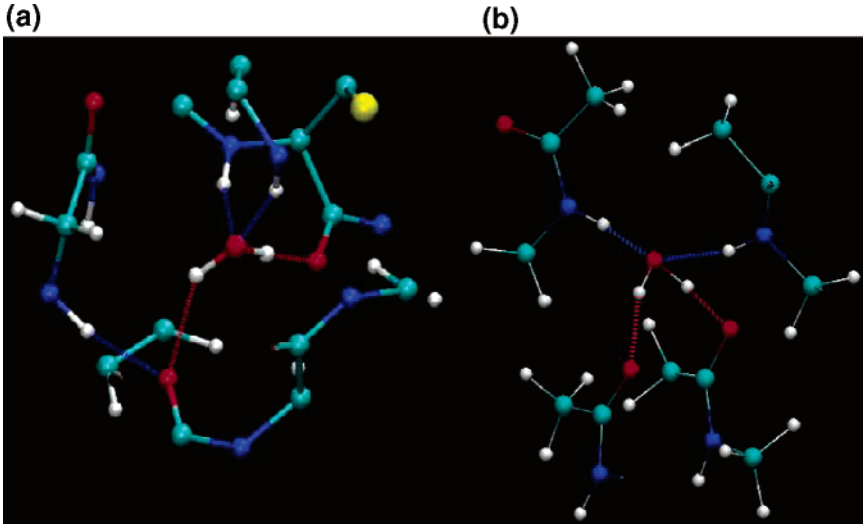

Figure 10. (a) Buried water in BPTI protein and (b) a water molecule hydrogen-bonded to four NMA molecules

NMA concentrations (0.9 and 0.8 MF) most of the water molecules exist either in isolation or in dimers or trimers. As the NMA concentration decreases larger water clusters appear but in chainlike rather than globular form. At 0.7 MF less than 5% of the water molecules accept two hydrogen bonds; thus clearly linear structures will dominate. In the midrange concentrations longer branched chains and small areas of tetrahedral water structure appear. As the NMA fraction decreases, the proportion of water molecules accepting two hydrogen bonds from other water molecules increases, reaching nearly 50% at 0.2 MF.

4. Conclusions

Classical MD simulations of aqueous NMA across the entire concentration range have been performed to investigate the solution structure of this simple peptidic fragment. Our results show that the water structure of aqueous NMA solutions is significantly different from that of pure water even at low NMA concentrations. At concentrations below 0.4 MF the water molecules continue to form large, percolating networks, topologically "string"-like, with one donated and one accepted strong hydrogen bond instead of a four-coordinated tetrahedral structure. As the NMA concentration is increased the water molecules become increasingly isolated into short linear clusters. Above 0.7 MF the majority of water molecules are either completely isolated or form one-half of a dimer. In contrast, NMA molecules show significant self-association even at the lowest concentrations explored. As water is added to pure NMA the hydrogen-bonded intermolecular NMA chains tend to break up at linear sections rather than at branch points. There is also an unexpected increase in short peptide oxygen separation distances on hydration that is due to water molecules forming hydrogen-bonded "bridges" between NMA molecules. A previously reported inequality in the hydrogen-bonding capabilities of the NMA methyl groups is herein explained. Due to the shape of the *trans*-NMA molecule the methyl group attached to the carbonyl group is likely to be pointed toward the carbonyl group belonging to the hydrogen-bond-accepting neighboring molecule. We find that one of the H_C methyls tends to be consistently pointed toward the oxygen of the neighboring NMA. The H_N methyl hydrogens show no such directionality. Given these observations, our aim is now to elucidate the respective contributions of energetic and entropic driving forces to this hydration process.

The hydrogen bonding and isolated water motifs present in aqueous NMA solutions and described in this paper are known to be of importance in real biological systems. In particular, this model system may lead to insights into the process of β-sheet formation in proteins. We also intend to further exploit the properties of this model system and its relevance to aqueous proteins and long-chain peptides by complementing this static structural survey with a detailed investigation into the dynamics of the system.

Acknowledgment. We thank Engineering and Physical Sciences Research Council for funding as well as Troy Whitfield and Raphael Troitzsch for advice and use of their analysis code. S.K.A. thanks Felix Fernandez-Alonso for useful discussions and Peter Rossky for helpful comments on the manuscript.

Supporting Information Available: Intermolecular medium-range structure and interactions of the methyl groups in liquid NMA. This material is available free of charge via the Internet at http://pubs.acs.org.

References and Notes

(1) Pauling, L.; Corey, R. B.; Branson, H. R. *Proc. Natl. Acad. Sci. U.S.A.* **1951**, *37*, 205.
(2) Guo, H.; Karplus, M. *J. Phys. Chem.* **1994**, *98*, 7104.
(3) Koddermann, T.; Ludwig, R. *Phys. Chem. Chem. Phys.* **2004**, *6*, 1867.
(4) Schellman, J. C. *C. R. Trav. Lab. Carlsberg, Ser. Chim.* **1955**, *29*, 230.
(5) Klotz, I. M.; Franzen, J. S. *J. Am. Chem. Soc.* **1962**, *84*, 3461.
(6) Kauzmann, W. *Adv. Protein Chem.* **1959**, *14*, 1.
(7) Huelsekopf, M.; Ludwig, R. *Magn. Reson. Chem.* **2001**, *39*, S197.
(8) Ludwig, R.; Weinhold, F.; Farrar, T. C. *J. Phys. Chem. A* **1997**, *101*, 8861.
(9) Schweitzer-Stenner, R.; Sieler, G.; Mirkin, N. G.; Krimm, S. *J. Phys. Chem. A* **1998**, *102*, 118.
(10) Whitfield, T. W.; Martyna, G. J.; Allison, S. K.; Bates, S. P.; Crain, J. *Chem. Phys. Lett.* **2005**, *414*, 210.
(11) Whitfield, T. W.; Martyna, G. J.; Allison, S. K.; Bates, S. P.; Vass, H.; Crain, J. *J. Phys. Chem. B* **2006**, *110*, 3624.
(12) Schmidt, J. R.; Corcelli, S. A.; Skinner, J. L. *J. Chem. Phys.* **2004**, *121*, 8887.
(13) Kwac, K.; Cho, M. *J. Chem. Phys.* **2003**, *119*, 2247.
(14) Kwac, K.; Cho, M. *J. Chem. Phys.* **2003**, *119*, 2256.
(15) Mantz, Y.; Gerrard, H.; Iftimie, R.; Martyna, G. J. *J. Am. Chem. Soc.* **2004**, *126*, 4080.
(16) Zhang, R.; Li, H.; Lei, Y.; Han, S. *J. Phys. Chem. B* **2004**, *108*, 12596.
(17) Zhang, R.; Li, H.; Lei, Y.; Han, S. *J. Mol. Struct.* **2004**, *693*, 17.

(18) Zhang, R.; Li, H.; Lei, Y.; Han, S. *J. Phys. Chem. B* **2005**, *109*, 7482.

(19) Williams, M. A.; Goodfellow, J. M.; Thornton, J. M. *Protein Sci.* **1994**, *3*, 1224.

(20) Smith, W.; Forester, T. *J. Mol. Graphics* **1996**, *14*, 136.

(21) MacKerell, A. D., Jr.; Bashford, D.; Bellott, R. L.; Dunbrack, R. L., Jr.; Evanseck, J. D.; Field, M. J.; Fischer, S.; Gao, J.; Guo, H.; Ha, S.; Joseph-McCarthy, D.; Kuchnir, L.; Kuczera, K.; Lau, F. T. K.; Mattos, C.; Michnick, S.; Ngo, T.; Nguyen, D. T.; Prodhom, B.; Reiher, W. E., III.; Roux, B.; Schlenkrich, M.; Smith, J. C.; Stote, R.; Straub, J.; Watanabe, M.; Wiorkiewicz-Kuczera, J.; Yin, D.; Karplus, M. *J. Phys. Chem. B* **1998**, *102*, 3586.

(22) Levitt, M.; Hirschberg, M.; Sharon, R.; Laidig, K,; Daggett, V. *J. Phys. Chem. B* **1997**, *101*, 5051.

(23) Whitfield, T.; Crain, J.; Martyna, G. J. *J. Chem. Phys.***2006**, *124*, 094503.

(24) Victor, P. J.; Hazra, D. K. *J. Chem. Eng. Data* **2002**, *47*, 79.

(25) Allison, S. K.; Fox, J.; Hargreaves, R.; Bates, S. P. *Phys. Rev. B* **2005**, *71*, 1.

(26) Dougan, L.; Bates, S. P.; Hargreaves, R.; Fox, J. P.; Crain, J.; Finney, J. L.; Reat, V.; Soper, A. K. *J. Chem. Phys.* **2004**, *121*, 6456.

(27) Mezei, M.; Beveridge, D. L. *J. Phys. Chem.* **1981**, *74*, 622.

(28) Soper, A. K.; Bruni, F.; Ricci, M. A. *J. Chem. Phys.* **1997**, *106*, 247.

(29) Denisov, V.; Venu, K.; Peters, J.; Hörlein, H. D.; Halle, B. *J. Phys. Chem. B* **1997**, *101*, 9380

(30) Steiner, T.; Desiraju, G. R. *Chem. Commun.* **1998**, *8*, 891.